ORIENTAL JOURNAL OF CHEMISTRY
An International Open Access, Peer Reviewed Research Journal
www.orientjchem.org
ISSN: 0970-020 X
CODEN: OJCHEG
2026, Vol. 42, No.(1):
Pg. 129-138

Development and Characterization of Biogenic Aurum Nanoparticles from a Southeast Asian Herb with Antioxidant Potential

ATIKAH MOHD NASIR[1]*, NURIN HAZIQAH RAZALI[1] and NURHANI ABDUL AZIZ[2]

[1]Centre of Diagnostic, Therapeutic and Investigative Studies, Faculty of Health Sciences, Universiti Kebangsaan Malaysia, Jalan Raja Muda Abdul Aziz, 50300 Kuala Lumpur, Malaysia
[2]Science Forensic Programme, Faculty of Health Sciences, Universiti Kebangsaan Malaysia, 43600 Bangi, Selangor
*Corresponding Author: atikahnasir@ukm.edu.my

http://dx.doi.org/10.13005/ojc/420113

(Received: December 09, 2025; Accepted: February 20, 2026)

ABSTRACT

This study explores the sustainable synthesis of Aurum nanoparticles (AuNPs) using Biokesum®, a Southeast Asian Herb called *Polygonum minus* leaves extract serves as both reducing and capping agent. Ultraviolet visible spectroscopy confirmed surface plasmon resonance peaks at 530–545 nm indicating well-formed AuNPs. Dynamic light scattering and zeta potential analysis revealed hydrodynamic diameters of 66 to 112 nm and moderate stability from –8.88 to –20 mV, respectively. Transmission electron microscopy and field emission scanning electron microscopy paired with energy dispersive spectroscopy revealed the morphology of AuNPs is spherical to quasi-spherical particles less than 20 nm, with phytochemical capping evidenced by carbon and oxygen signatures. X-ray fluorescence analysis confirmed the successful formation of AuNPs by identifying and quantifying a significant amount of AuNPs, residual chloride, and trace phytochemical. Antioxidant assays (DPPH) revealed pH-dependent activity, with maximal activity at pH 4 (~35%), while Biokesum® extract (~95%) and quercetin (~97%) maintained consistently high activity across all pH values. Sample A5 (66 nm, –14.6 mV) emerged as the most optimal formulation. These findings highlight Biokesum® as an effective, eco-friendly alternative for AuNPs synthesis for biomedical and pharmaceutical applications.

Keywords: Green synthesis; Aurum nanoparticles (AuNPs); *Polygonum Minus*; Phytochemical capping; Antioxidant activity.

INTRODUCTION

Oxidative stress results from an imbalance between reactive oxygen species (ROS) generation and endogenous antioxidant defences. This imbalance plays a central role in cellular damage and the progression of chronic diseases such as cardiovascular disorders, neurodegeneration, diabetes, and cancer [1]. Environmental pollutants and modern lifestyle factors further elevate ROS

levels, emphasizing the need for effective antioxidant agents. Although natural antioxidants mitigate ROS by donating electrons to stabilize reactive species[2],their therapeutic use is limited by instability, low solubility, and susceptibility to degradation [3].

Nanomaterials have gained increasing attention as alternative antioxidants because of their high surface-to-volume ratios, tunable physicochemical properties, and intrinsic redox activities. Organic nanomaterials, metal oxides, and noble metal nanoparticles including Aurum nanoparticles (AuNPs) exhibit radical scavenging and enzyme-mimetic behaviors [4,5]. AuNPs are particularly attractive for biomedical applications because of their biocompatibility, stability, and low toxicity [6]. However, conventional AuNP synthesis often requires hazardous chemicals and energy-intensive procedures, limiting sustainability.

Green nanotechnology addresses these limitations by utilizing phytochemicals as reducing and stabilizing agents, enabling eco-friendly and cost-effective nanoparticle production[7]. *Polygonum minus*also known as kesum, a Southeast Asian herb rich in phenolic acids, flavonoids, and terpenoids, exhibits antioxidant, anti-inflammatory, antimicrobial, and anticancer properties[8,9]. Its abundant flavonoids contribute significantly to these bioactivities[10] and standardized extracts such as Biokesum® serve to further validate its functional potential[11]. Nevertheless, phytochemical instability and low bioavailability limit direct therapeutic application[12].

Therefore, this study aims to develop biogenic AuNPs using Biokesum® leaf extract through an environmentally friendly synthesis approach and to comprehensively characterize the resulting nanoparticles in terms of their optical properties, particle size distribution, surface charge, morphology, and elemental composition. In addition, the antioxidant potential of the synthesized AuNPs is evaluated under different pH conditions to elucidate their functional performance. By correlating physicochemical characteristics with bioactivity outcomes, this work seeks to establish the structure–stability–antioxidant relationship of Biokesum®-derived AuNPs and to highlight their promise as sustainable nanomaterials for biomedical and pharmaceutical applications.

MATERIALS AND METHODS

Materials

Aurum (III) chloride trihydrate, $AuCl_4H_7O_3$ (99.9%) purchased from Shanghai Macklin Biochemical. The *Polygonum minus* water extracts used in this study were from Biotropics Malaysia under the trade names of Biokesum*®* (batch number: KE 220103). Biokesum*®* is a water extract of the leaves of *Polygonum minus,* standardized based on a specification of not less than 0.45% of quercetin-3-glucuronide and not less than 100 mg GAE/g dE total phenolic content. The high-performance liquid chromatography (HPLC) fingerprint of Biokesum*®* was obtained according to the HPLC-diode array detection method using a Kinetex 1.7 µm C18 column (2.1 × 150 mm). The mobile phase consisted of solvent A: 0.10% formic acid in water and B: 0.10% formic acid in acetonitrile mixed according to a linear gradient program with a flow rate of 0.4mL/min. The solvent composition was set to 11% B from t= 0-18 min followed by 95% B from t = 20-23 min, before final t = 25 min at 11% B. Injection volume was 2.0 µl and the chromatogram was recorded at 366 nm.

Preparation of Stock Solutions

Initially, an Au precursor stock solution of 1 mM $AuCl_4H_7O_3$ was prepared by mixing 39.383 mg into 100 mL of pure deionized water (HPLC grade) to ensure purification. The Au precursor stock solution was labelled and stored in an aluminium wrap Schott bottle at 4°C until further use. Biokesum*®* stock solution (0.1%) was prepared by adding 0.1g of powdered Biokesum*®* into 100ml deionized water. The mixture was stirred slowly for 10 min to form a homogeneous solution. Later, this stock solution was filtered by a Teflon membrane 0.04 µm to remove any impurities. Finally, the filtrate was labelled and kept in a Schott bottle at 4°C until further use. The stock solutions of Au precursor and Biokesum® were used as control solutions to monitor the production of AuNP colloidal solutions. Both of the stock solutions were labelled as Control 1 and Control 2, respectively.

Synthesis of AuNPs

To study the ability of Biokesum*®* extract as a bioreducing agent to produce AuNPs, various volumes of Biokesum*®* extract were used using a fixed volume of 1 mM $AuCl_4H_7O_3$. A total of 5 mL

of $AuCl_4$ stock solution was added dropwise to a set of volumes of Biokesum® extract solution as determined in Table 1. The solution mixture was stirred continuously using a magnetic stirrer at room temperature. Initial observations were recorded through the color change of the solution from pale yellow to purple, then to ruby red. The formation of AuNPs colloidal solution was considered occurred when the mixed solution changed from pale yellow to purple to ruby red. The colour change can be observed with the naked eye. Further analysis was performed using an ultraviolet visible (UV-VIS) spectroscopy technique with a wavelength range of 400 to 800 nm. All experiments were performed in triplicate to verify the validity.

Table 1: Formulation parameters for Au nanoparticle synthesis using Biokesum® extract

Sample	Volume 1 mM $AuCl_4H_7O_3$	Volume 0.1% Polygonum stock solution minus	Ratio of $ACl_4H_7O_3$ Polygonum minus
Control 1	5	0	5:0
Control 2	0	5	0:5
A1	5	1	5:1
A2	5	2	5:2
A3	5	3	5:3
A4	5	4	5:4
A5	5	5	5:5
A6	5	6	5:6

Characterization of AuNPs

AuNPs formation was monitored using an ultraviolet/visible/near infrared spectrometer (Perkin Elmer Lambda 950) over 400–800 nm at 1 nm intervals with deionized water as baseline. Hydrodynamic diameter and zeta potential were measured with a nanoparticle size analyzer (Malvern Zetasizer Nano ZS, measurement range 0.3 nm–10 µm, zeta potential range –150 mV to +150 mV) after dilution in deionized water at 25 °C in triplicate. Transmission electron microscopy (TEM) was performed on a Talos L120C microscope (120 kV, 0.2 nm resolution, 35×–910× magnification) by dropcasting the colloid onto carboncoated copper grids. Field emission scanning electron microscopy coupled with energydispersive Xray spectroscopy was carried out on a ZEISS MERLIN field emission scanning electron microscope at 15 kV with elemental mapping. Xray fluorescence analysis of lyophilized nanoparticle powder was conducted on a Rigaku ZSX Primus IV wavelength dispersive Xray fluorescence spectrometer.

Radical Scavenging Activity

The antioxidant activity of the 2,2-diphenyl-1-picrylhydrazyl (DPPH) method was used to evaluate the radical scavenging activity of AuNPs. The dark purple DPPH free radical changed to a yellow stable molecule when the electrons of the DPPH free radical interact with the hydrogen of the free radical scavenging antioxidant. Therefore, the degree of DPPH color change can indicate the antioxidant scavenging potential of the extract. To measure the antioxidant activity, the decrease in color intensity was monitored over time at a wavelength of 517 nm. This wavelength corresponds to the strongest absorption for DPPH.All measurements were performed in triplicate.

Cytotoxicity Assay

V79-4 cells were cultured in DMEM supplemented with 10% FBS, 1 mM sodium pyruvate and 1% antibiotics, and maintained at 37 ± 1 °C in 5 ± 1% CO_2. Confluent cells were detached by trypsinisation, counted, and seeded into 96-well plates at 10,000 cells/well, then incubated for at least 12 hours to reach 70–80% confluency. The test item was sterilised by 0.2 µm filtration, prepared at 50% v/v, and serially diluted to obtain additional concentrations of 25%, 12.5%, 6.25%, 3.13% and 1.56% v/v. Cells were exposed to each concentration in triplicate for 24 h ± 30 min under standard incubation conditions. After exposure, 5 mg/ml MTT solution was added to each well and incubated for 4

h ± 30 min, followed by removal of the reagent and solubilisation of the formazan crystals. Absorbance was measured to determine cell viability.

RESULTS AND DISCUSSION

HPLC Chromatogram Analysis of Biokesum® and Reference Standards

The HPLC analysis of Biokesum® (Figure 1a) revealed two major peaks corresponding to quercetin-3-O-glucuronide and quercitrin, as confirmed by comparison with retention times (RT) of authentic standards (Figure 1b). The elution profiles of these compounds in Biokesum® (RT 7.332 min and 14.632 min) closely align with those of the standards (RT 7.335 min and 14.597 min), strongly supporting their identification. Retention time matching is a widely accepted method for preliminary compound identification in HPLC[13]. The minor discrepancies in retention times (~0.003–0.035 min) are likely due to slight variations in experimental conditions such as column temperature or mobile phase composition[14].

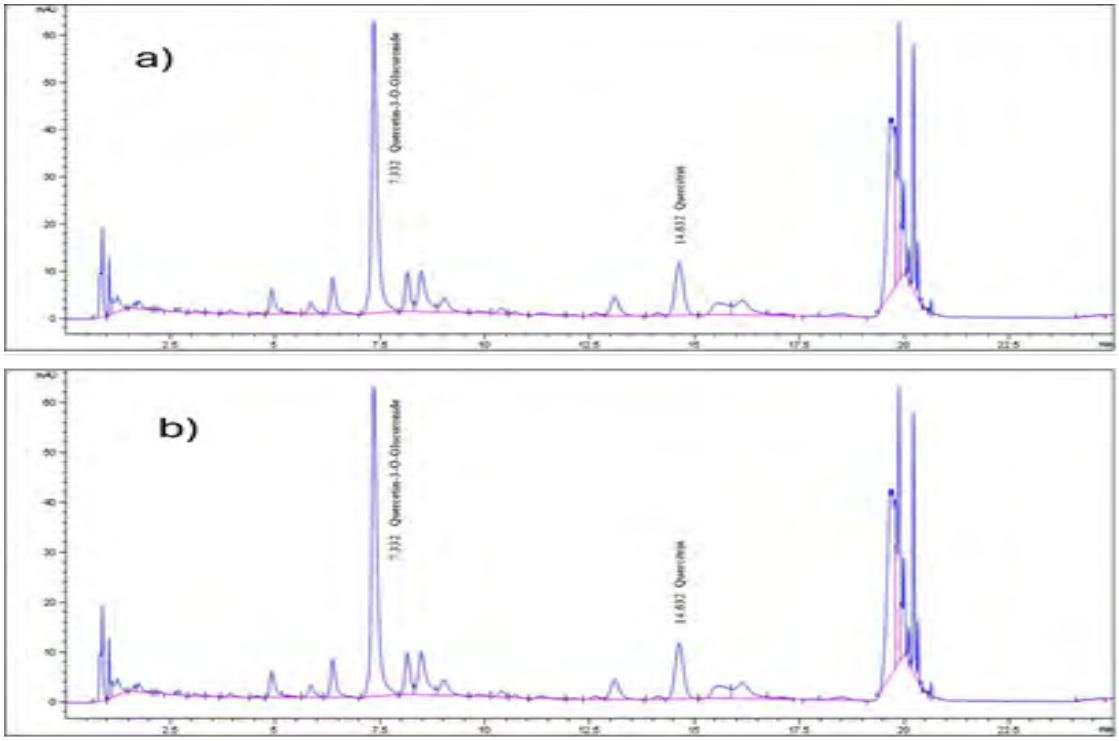

Fig. 1: High-performance liquid chromatography (HPLC) chromatogram of Biokesum® extract and reference standards; (a) Biokesum® chromatogram showing quercetin-3-O-glucuronide (RT 7.332 min) and quercitrin (RT 14.632 min). (b) Reference standards of quercetin-3-O-glucuronide (RT 7.335 min) and quercitrin (RT 14.597 min)[12].

The quantification of quercetin-3-O-glucuronide (1.3%) and quercitrin (0.4%) in Biokesum® highlights the significant presence of these bioactive flavonoids. Quercetin derivatives, particularly glucuronides, are renowned for their antioxidant and anti-inflammatory properties, as demonstrated in preclinical models[15]. Additionally, glucuronidation often enhances solubility and bioavailability, as observed in pharmacokinetic studies of quercetin derivatives[16], suggesting that Biokesum® could offer improved in vivo efficacy. The identified concentrations (1.3% and 0.4%) are pharmacologically relevant, as similar levels of quercetin glycosides in plant extracts have demonstrated bioactivity in reducing oxidative stress [17]. However, the presence of unresolved minor peaks in the chromatogram (Figure 1a) implies that

other phytoconstituents, such as phenolic acids or additional flavonoids, may contribute synergistically to Biokesum®'s bioactivity.

Ultraviolet-visible Spectrum and Surface Plasmon Resonance (SPR) Analysis

The successful biosynthesis of AuNPs was confirmed using ultraviolet-visible (UV-Vis) spectroscopy (Figure 2a), which detects the characteristic surface plasmon resonance (SPR) band arising from the oscillation of surface electrons[18]. All samples (A2–A6) showed distinct surface plasmon resonance (SPR) peaks between 534 to 568 nm (Figure 2b), indicating the reduction of $Au^{3}{}_{2}$ to Au_{2} and the formation of spherical or quasi-spherical nanoparticles.A systematic blue shift in the surface plasmon resonance maximum was observed with increasing Biokesum® extract concentration, shifting from 568 nm (A2) to 534 nm (A6). This progressive shift toward shorter wavelengths is a well-established indicator of reduced average particle size [19]. The sharp, intense, and symmetric peak observed for samples A4 to A6 suggests the formation of small, monodisperse, and well-stabilized nanoparticles.

This result can be attributed to the high content of bioactive phytochemicals in Biokesum®, particularly quercetin derivatives, which act as strong reducing and capping agents [17,20]. At the optimal concentration in A6, these compounds promote rapid nucleation and effective surface passivation, preventing ripening and aggregation [21]. In contrast, lower extract concentrations (A2, A3) produced broader, weaker peaks at 565–568 nm, indicating polydispersity, possible aggregation, and incomplete reduction due to limited reducing agents[5,7]. The absence of secondary peaks in A4–A6 confirms minimal anisotropic structures or aggregation[22]. Similar trends were reported for *Zingiber officinale*-mediated AuNPs, where higher extract levels resulted in a blue shift and smaller particles[19]. Overall, extract concentration is a key determinant of nanoparticle size and stability, with A4-A6 representing the optimal Biokesum®- AuNPs ratio.

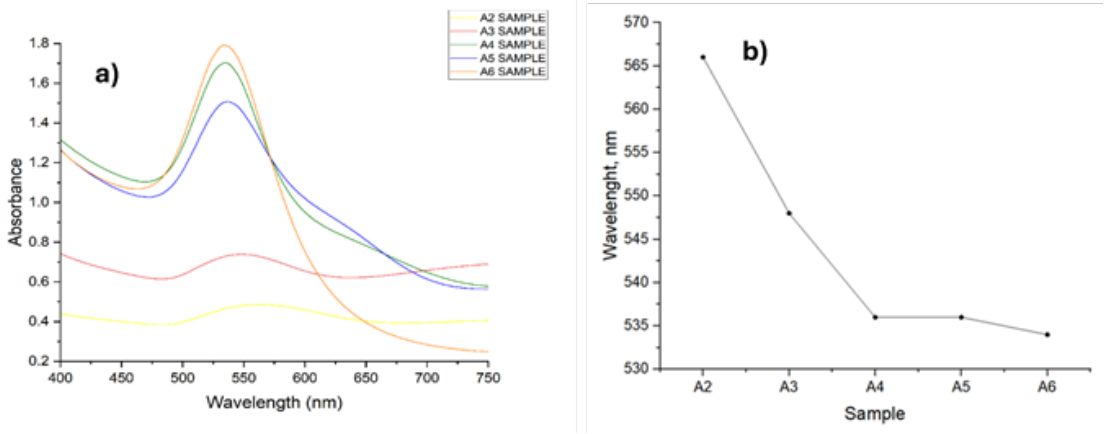

Fig. 2. a) Ultraviolet-visible (UV-Vis) absorption spectra of AuNPs synthesized with increasing Biokesum® extract volumes (samples A2–A6). b) Surface resonance resolution of synthesized AuNPs

Zeta Potential Analysis

As summarized in Table 2, dynamic light scattering (DLS) and zeta potentialcollectively provided key insights into colloidal stability and size distribution, demonstrating the strong influence of extract concentration on nanoparticle characteristics. Zeta potential analysis showed moderate stability for samples A5 (–14.6 mV) and A4 (–13 mV), though the values remained below the ±30 mV threshold associated with long-term stability[25]. Sample A6 (–8.88 mV) aggregated rapidly despite its small size, indicating that high Biokesum® concentrations enhance reduction but may yield insufficient surface passivation[26]. The relatively high zeta potential of sample A2 (–20 mV) likely reflects the presence of charged aggregates rather than stable nanoparticles. The stability trend (A5 > A4/A3 > A6 > A2) reflects

a balance between reduction kinetics and capping efficiency. Rapid nucleation at higher extract concentrations is facilitated by flavonoids such as quercetin-3-O-glucuronide[21], but excessive extract can saturate reduction sites without adequate surface stabilization. In contrast to the previous study, where increasing plant extract concentration led to red-shifted SPR bands indicative of nanoparticle aggregation[5], the present findings suggest that the distinct flavonoid composition of Biokesum® promotes efficient Au^{3+} reduction while exerting a differential influence on AuNPs stabilization dynamics. Overall, sample A5 represents the most promising formulation, balancing small size, monodispersed, and moderate stability.

High-Resolution Transmission Electron Microscopy (HRTEM) Analysis

Transmission Electron Microscopy (TEM) analysis of sample A5 revealed predominantly quasi-spherical, irregularly shaped nanoparticles, indicative of isotropic growth facilitated by plant-derived reducing and capping agents (Figure 3). The particles were well-dispersed with minor aggregation, likely due to partial surface capping or limited phytochemical stabilization, a phenomenon similarly observed in *Azadirachta indica*–mediated AuNPs[27]. The majority of nanoparticles measured below 20 nm, confirming their nanometric size and suitability for biomedical, catalytic, and environmental applications. These findings align with previous studies where *Hibiscus rosa-sinensis*–synthesized AuNPs exhibited sizes of 10–30 nm[28], while *Azadirachta indica*–derived nanoparticles averaged 36.4 nm[27].

Table 2: Stability characteristics of synthesized AuNPs based on DLS and zeta potential analyses

Sample	DLS Size (nm)	Zeta Potential (mV)
A6	67.65	-8.88
A5	66	-14.6
A4	105	-13.0
A3	112	-13.0
A2	250	-20.0

Field Emission Scanning Electron Microscopy with Energy-Dispersive X-ray (FESEM-EDX) Analysis

Figure 4 shows FESEM analysis of sample A5 revealed predominantly quasi-spherical, irregularly shaped nanoparticles that were relatively well-dispersed with slight aggregation, a common feature in plant-mediated green synthesis[27,28]. Elemental mapping confirmed dense Au distributions at particle sites, while carbon (C) and oxygen (O) were more homogeneously distributed, likely originating from Biokesum® phytochemicals acting as reducing and stabilizing agents. EDX spectra supported these observations, showing characteristic peaks for Au (~2.3 keV), C (~0.28 keV), and O (~0.52 keV), consistent with typical biosynthesized AuNPs. These findings align with previous reports indicating that green-synthesized AuNPs are coated with plant-derived organic molecules, which enhance stability

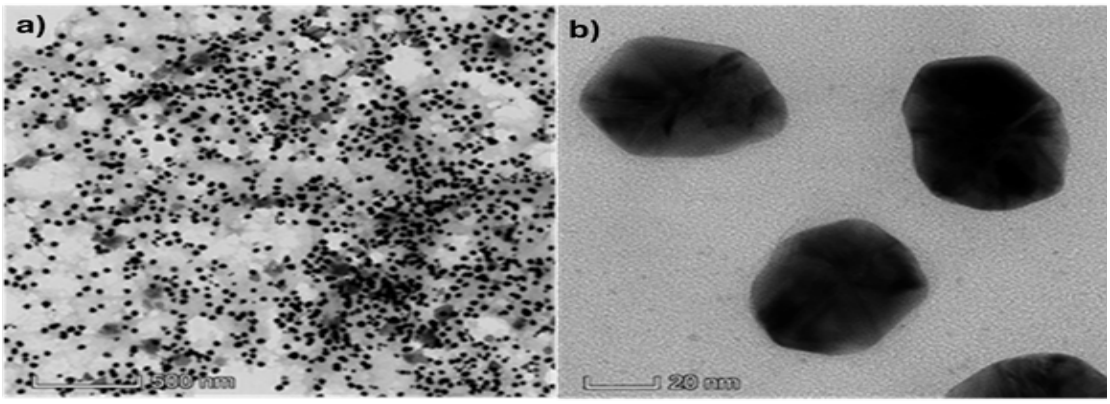

Fig. 3: Transmission electron microscopy (TEM) images of sample A5 AuNPs (Talos L120C, 120 kV). (a) Particle distribution (500 nm scale). (b) Quasi-spherical morphology with sizes below 20 nm (20 nm scale)

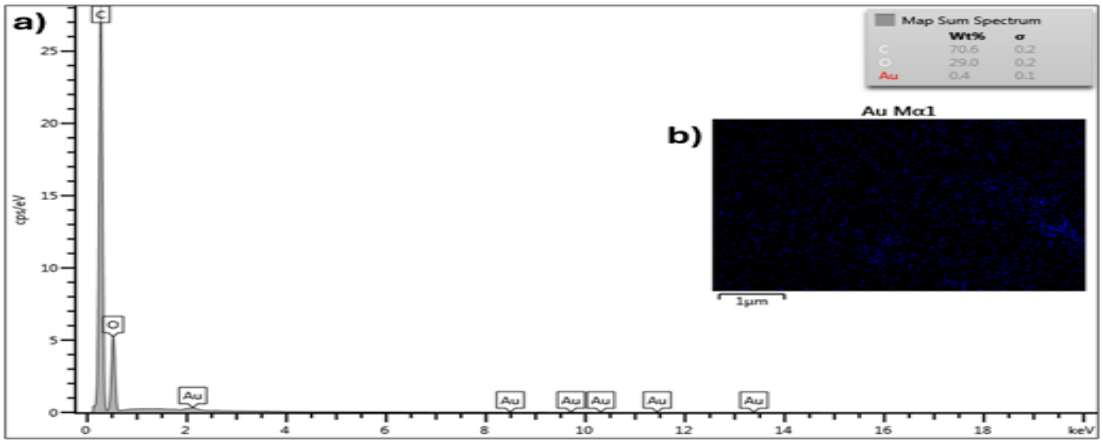

Fig. 4: Field-emission scanning electron microscopy with energy-dispersive X-ray spectroscopy (FESEM-EDX) of sample A5. (a) EDX spectrum showing Au and (b) individual elemental distribution of Au.

and prevent aggregation[27,28]. Overall, the results confirm that Biokesum® effectively facilitated the green synthesis of nanoscale AuNPs with good dispersion and biomolecule capping.

X-ray Fluorescence (XRF) Analysis

X-ray fluorescence (XRF) analysis was conducted to confirm the elemental composition of the Biokesum® mediated AuNPs. The result of sample A5 indicated the presence of Au (intensity 4.6624), confirming the successful reduction of Au^{3+} precursor into elemental Au by Biokesum® extract. The residual Cl (intensity 0.2307) likely originates from incomplete reduction of the Au precursor, most commonly chloroauric acid ($HAuCl_2$), a typical feature in green synthesis[18]. Similar observations were reported by[19], where Zingiber officinale–mediated AuNPs retained Cl due to partial reduction. The trace Al, K, and S with intensity 0.1423, 0.1929 and 0.1510 respectively, are characteristic of phytochemicals and organic acids in plant extracts, supporting the role of biomolecules in capping and stabilizing the nanoparticles[29]. Although XRF does not provide oxidation state information, the confirmed presence of Au strongly supports nanoparticle formation, particularly when interpreted alongside complementary characterization techniques such as UV–Vis spectroscopy or XRD. Overall, the XRF findings verify that Biokesum® extract effectively facilitates the formation of Au nanoparticles while maintaining a relatively clean elemental profile, consistent with previously reported green synthesis approaches.

Antioxidant Activity Analysis (DPPH Assay)

Quercetin, a well-known flavonoid antioxidant, is most stable and effective in mildly acidic conditions[15]. Similarly, the biosynthesized AuNPs, sample A5 exhibited maximal DPPH scavenging (~35%) at pH 4, likely because the Biokesum®-derived phytochemical capping remains protonated and can donate hydrogen atoms to neutralize radicals. From Figure 5, at pH 5 and 7, activity dropped sharply (~17–19%), possibly due to deprotonation of phenolic groups and changes in nanoparticle surface charge, rather than quercetin degradation, which occurs only above pH 9[30]. Under moderately alkaline conditions (pH 9–11), activity increased slightly (~19–23%), reflecting enhanced nanoparticle formation and greater surface area for biomolecule adsorption. At pH 13, scavenging dropped drastically (~6.5%) due to phytochemical degradation or desorption, consistent with flavonoid instability under strong alkalinity [31]

In contrast, Biokesum® extract (~95%) and quercetin (~97%) maintained high antioxidant activity across all pH levels, highlighting their inherent stability. The lower activity of AuNPs aligns with reports that plant metabolites consumed during Au^3_2 reduction reduce the available pool of bioactive compounds[20]. However, some studies report higher AuNPs activity than crude extracts, depending on phytochemical capping and synthesis conditions[22]. Overall, these results demonstrate

that pH significantly influences the antioxidant performance of Biokesum®-mediated AuNPs, with mildly acidic conditions favoring maximal activity, moderate alkalinity supporting nanoparticle formation, and extreme alkalinity compromising stability.

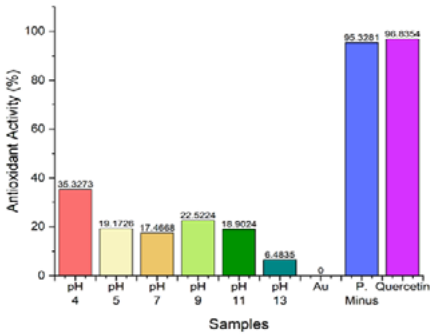

Fig. 5. DPPH radical scavenging activity of sample A5, Biokesum® extract, and quercetin standard

Cytotoxicity Evaluation of Biokesum® on V79-4 Cells

The cytotoxicity of sample A5 was evaluated using the MTT assay on V79-4 fibroblast cells to assess biocompatibility (Table 3). Cell viability after 24 h exposure to Biokesum® (1.56–50 % v/v) remained high, ranging from 101% to 87%, with no treatment falling below the ISO 10993-5 cytotoxicity threshold of 70% (ISO 10993-5:2009). The MTT assay measures mitochondrial activity via reduction of MTT to formazan, reflecting cellular metabolic integrity. These results indicate that Biokesum® does not interfere with mitochondrial function, consistent with reports for green-synthesized AuNPs capped with plant-derived biomolecules, which typically maintain >80 % viability[19,22].

The non-cytotoxicity may be attributed to flavonoids such as quercetin-3-O-glucuronide and quercitrin, which scavenge ROS and protect cells

Table 3: V79-4 cell viability after 24-hour exposure to sample A5

		Optical Density, OD (570 nm)					
		Replicate 1	Replicate 2	Replicate 3	Average	Standard Deviation (SD)	Cell Viability (%)
Negative Control Test	3.214	3.051	3.032	3.099	0.10	100	
	1.56	2.999	3.119	3.269	3.129	0.14	101
Item	3.13	3.452	3.426	2.822	3.233	0.36	104
Concentration	6.25	3.341	3.443	2.911	3.232	0.28	104
n (% v/v)	12.5	2.716	2.878	2.660	2.751	0.11	89
	25	2.919	2.788	2.897	2.868	0.07	93
	50	2.709	2.719	2.679	2.702	0.02	87
Positive Control(10 mM)		0.184	0.186	0.165	0.178	0.01	6

from oxidative stress[15,17]. These phytochemicals also serve as nanoparticle capping agents, reducing membrane interactions and potential oxidative or inflammatory responses. Potential optical interference from AuNPs in the MTT assay is noted, and complementary assays (LDH release, Neutral Red uptake, Annexin V/PI staining) are recommended to confirm viability.

Overall, the A5 formulation, with stable size (66 nm, −14.6 mV) and moderate antioxidant activity, is non-cytotoxic and biocompatible, supporting its safe application in nanobiotechnology. These findings align with other green AuNP systems, such as Zingiber officinale and Azadirachta indica, which demonstrate high cellular viability and low inflammatory potential[19,27].

CONCLUSIONS

In conclusion, this study demonstrates that Biokesum® is an effective bio-reducing

and stabilizing agent for the green synthesis of AuNPs. Its rich phytochemical content, particularly quercetin derivatives, enabled the formation of nanoparticles with defined morphological and optical characteristics. Characterization by UV-Vis, DLS, zeta potential, TEM, and FESEM-EDX showed that sample A5 achieved an optimal balance of particle size (~66 nm), surface plasmon resonance (~530–535 nm), and moderate colloidal stability (–14.6 mV), making it the most promising formulation. The AuNPs exhibited pH-dependent antioxidant activity, with maximal DPPH scavenging at acidic pH (4) and decreased efficacy at neutral and highly alkaline conditions. In contrast, Biokesum® extract and quercetin maintained high activity (>95%), indicating that phytochemical consumption during nanoparticle synthesis limits free radical scavenging. Overall, Biokesum®-mediated AuNPs offer a sustainable, biocompatible platform with potential for mitigating oxidative stress-related disorders. Challenges such as moderate stability and variable antioxidant performance warrant further optimization through surface functionalization, long-term stability assessment, and in vivo validation. Future studies should refine synthesis parameters, enhance stability using polymeric or biomolecular coatings, and evaluate pharmacological safety and efficacy in relevant biological models.

ACKNOWLEDGEMENTS

We would like to express our gratitude to the Universiti Kebangsaan Malaysia, Selangor, Malaysia for the Geran Galakan Penyelidik Muda (GGPM) code GGPM-2023-039 and Geran Galakan Fakulti Sains Kesihatan NN-2025-037.

REFERENCES

1. Sies, H., Berndt, C., Jones, D. P., Annual Review of Biochemistry, **2017**, 86, 715–748.
2. Pham-huy, L. A., He, H., Pham-huy, C., International Journal of Biomedical Science, **2008**, 4, 89–96.
3. Muscolo, A., Mariateresa, O., Giulio, T., Mariateresa, R., International Journal of Molecular Sciences, **2024**, 25, 3264.
4. Ge, X., Cao, Z., Chu, L., Antioxidants, **2022**, 11, 791.
5. Singh, S., Frontiers in Chemistry, 2019, 7, 1–10.
6. Dykman, L. A., Khlebtsov, N. G., Chemical Science, **2017,** 8, 1719–1735.
7. Pattoo, T. A., Plant Science Archives, **2023**, 8, 12.
8. Christapher, P., Parasuraman, S., Christina, J., Asmawi, M. Z., Vikneswaran, M., Pharmacognosy Research, 2015, 7, 1–6.
9. Seimandi, G., Álvarez, N., Stegmayer, M. I., Fernández, L., Ruiz, V., Favaro, M. A., Derita, M., Molecules, **2021**, 26, 5956.
10. Al-Snafi, P. D. A. E., IOSR Journal of Pharmacy, **2017,** 7, 21–32.
11. Williams, M., Jenks, A., HerbalGram, 2024, 139, 6–12.
12. Chinnappan, S. M., George, A., Choudhary, Y. K., Godavarthi, A., Teng, C. L., Jin, W. H., Current Traditional Medicine, **2022**, 9.
13. Arumugam, B., Manaharan, T., Heng, C. K., Kuppusamy, U. R., Palanisamy, U. D., LWT – Food Science and Technology, **2014,** 59, 707–712.
14. Popovici, L. F., Brinza, I., Gatea, F., Badea, G. I., Vamanu, E., Oancea, S., Hritcu, L., Antioxidants, **2025**, 14, 97.
15. Azeem, M., Hanif, M., Mahmood, K., Ameer, N., Chughtai, F. R. S., Abid, U., Polymer Bulletin, **2023**, 80, 241–262.
16. Hai, Y., Zhang, Y., Liang, Y., Ma, X., Qi, X., Xiao, J., Xue, W., Luo, Y., Yue, T., Food Frontiers, **2020,** 1, 420–434.
17. Alharbi, H. O. A., Alshebremi, M., Babiker, A. Y., Rahmani, A. H., Biomolecules, **2025**, 15.
18. Ghosh, S. K., Pal, T., Chemical Reviews, **2007**, 107, 4797–4862.
19. Fouda, A., Eid, A. M., Guibal, E., Hamza, M. F., Hassan, S. E. D., Alkhalifah, D. H. M., El-Hossary, D., Applied Sciences, **2022**, 12.
20. Huang, X., Devi, S., Bordiga, M., Brennan, C. S., Xu, B., International Journal of Food Science & Technology, **2023,** 58, 1673–1694.
21. Azam, A., Revista Electronica De Veterinaria, **2024,** 25, 3576–3584.
22. dos Santos Corrêa, A., Contreras, L. A., Keijok, W. J., Barcelos, D. H. F., Pereira, A. C. H., Kitagawa, R. R., Scherer, R., de Oliveira Gomes, D. C., da Silva, A. R., Endringer, D.

C., de Oliveira, J. P., Guimarães, M. C. C., 22. Materials Science and Engineering C, **2018,** 91, 853–858.
23. María, A., Nogales, J., University of the Basque Country, **2024,** 2024.
24. Pratap, D., Soni, S., Plasmonics, **2021**, 1495–1513.
25. Dissanayake, K., Midekessa, G., Godakumara, K., Ord, J., Viil, J., La, F., Kopanchuk, S., Rinken, A., Andronowska, A., Bhattacharjee, S., Rinken, T., Fazeli, A., ACS Omega, **2020.**
26. Baek, W., Chang, H., Bootharaju, M. S., Kim, J. H., Park, S., Hyeon, T., JACS Au, **2021**, 1, 1849–1859.
27. Gopalakrishnan, V., Singaravelan, R., Inorganic Chemistry Communications**, 2023**, 158, 111609.
28. Kumar, B., Smita, K., Angulo, Y., Debut, A., Cumbal, L., Journal of Composites Science, **2022**, 6, 322.
29. Zhang, J., Cui, Y., Zhou, T., Wang, J., Zhu, Z., Liu, F., Xiao, G., Accreditation and Quality Assurance, **2023,** 28, 299–310.
30. Kellil, A., Grigorakis, S., Loupassaki, S., Makris, D. P., Applied Sciences, **2021**, 11, 2579.
31. Jurasekova, Z., Domingo, C., Garcia-Ramos, J. V., Sanchez-Cortes, S., Physical Chemistry Chemical Physics, **2014**, 16, 12802–12811.